Leukemia Inhibitory Factor: A Newly Identified Metastatic Factor in Rhabdomyosarcomas

Marcin Wysoczynski,[1] Katarzyna Miekus,[1] Kacper Jankowski,[1] Jens Wanzeck,[1] Salvatore Bertolone,[1] Anna Janowska-Wieczorek,[2] Janina Ratajczak,[1] and Mariusz Z. Ratajczak[1,3]

[1]James Graham Brown Cancer Center, University of Louisville, Louisville, Kentucky; [2]Department of Medicine, University of Alberta, Edmonton, Alberta, Canada; and [3]Department of Physiology, Pomeranian Medical University, Szczecin, Poland

Abstract

Rhabdomyosarcoma frequently infiltrates bone marrow and this process involves the stromal-derived factor-1 (SDF-1)–CXCR4 axis. Because leukemia inhibitory factor (LIF), like SDF-1, is secreted by bone marrow stroma and directs the regeneration of skeletal muscles, we examined whether the LIF–LIF receptor (LIF-R) axis affects the biology of rhabdomyosarcoma cells. We found that in rhabdomyosarcoma cells, LIF stimulates the following: (*a*) phosphorylation of mitogen-activated protein kinase p42/44, AKT, and signal transducers and activators of transcription 3, (*b*) adhesion and chemotaxis, and (*c*) increased resistance to cytostatics. To compare the biological effects of LIF versus SDF-1, we examined the RH30 cell line, which is highly responsive to both ligands, and found that the chemotaxis of these cells is significantly reduced when the inhibitors of both receptors (T140 for CXCR4 and gp190 blocking antibody for LIF-R) are added simultaneously. Subsequently, by using repetitive chemotaxis to LIF or SDF-1, we selected from the RH30 line subpopulations of cells that respond to LIF but not SDF-1 (RH30-L) or to SDF-1 but not LIF (RH30-S). We found that (*a*) RH30-L cells seed better to the bone marrow, liver, and lymph nodes of immunodeficient mice than RH30-S cells and (*b*) mice inoculated i.m. with the RH30-L cells had more rhabdomyosarcoma cells in the bone marrow and lung after 6 weeks. Thus, we present the first evidence that the LIF–LIF-R axis may direct rhabdomyosarcoma metastasis. Further, because we showed that the *in vivo* metastasis of RH30 cells is inhibited by small interfering RNA against LIF-R, molecular targeting of this axis could become a new strategy to control the metastasis of rhabdomyosarcoma. [Cancer Res 2007;67(5):2131–40]

Introduction

Rhabdomyosarcoma is the most common soft-tissue sarcoma of adolescence and childhood and accounts for 5% of all malignant tumors in patients under 15 years of age (1–10). There are two major histologic subtypes of rhabdomyosarcoma, alveolar rhabdomyosarcoma (ARMS) and embryonal rhabdomyosarcoma (ERMS). Clinical evidence indicates that ARMS is more aggressive, has a significantly worse outcome than ERMS, and in almost all cases is associated with bone marrow involvement. Moreover, ARMS is characterized by the translocation t(2;13)(q35;q14) in 70% of cases or the variant t(1;13)(p36;q14) in a smaller percentage of cases. These translocations disrupt the *PAX3* and *PAX7* genes on chromosome 2 and 1, respectively, and the *FKHR* gene on chromosome 13, and generate *PAX3-FKHR* and *PAX7-FKHR* fusion genes (7–10). These fusion genes encode the fusion proteins PAX3-FKHR and PAX7-FKHR, believed to play a role in cell survival and dysregulation of the cell cycle in ARMS cells (1–10).

Why rhabdomyosarcoma cells metastasize to the bone marrow is still poorly understood. There is increasing evidence that bone marrow stroma secretes chemoattractants, which attract rhabdomyosarcoma cells into the bone marrow microenvironment where they find conditions favorable for survival and expansion. We and others showed that the α-chemokine stromal-derived factor-1 (SDF-1) and hepatocyte growth factor/scatter factor (HGF/SF) are secreted by bone marrow stroma and, along with their respective receptors CXCR4 and c-met, are expressed in rhabdomyosarcoma cells and play an important role in the metastasis of rhabdomyosarcoma (11–14). Although both SDF-1 and HGF chemoattracted rhabdomyosarcoma cells and enhanced their metastatic behavior (11, 14), surprisingly, blockage of both the SDF-1–CXCR4 and the HGF–c-met axes did not completely inhibit the chemotaxis of these cells to conditioned medium by bone marrow stroma or lymph nodes, suggesting the involvement of other chemoattractants as potential prometastatic factors in rhabdomyosarcoma.

Based on observations that the gp190 signaling cytokine, leukemia inhibitory factor (LIF), stimulates proliferation of skeletal muscle satellite cells and myocytes (15, 16), as well as cardiomyocytes (17), and that normal bone marrow stroma cells express and secrete LIF (18), we hypothesized that the LIF–LIF receptor (LIF-R) axis is such a prometastatic factor promoting the progression of rhabdomyosarcoma. Furthermore, because oncostatin M (OSM), another cytokine in the gp190 signaling family, also binds to LIF-R, we also examined the possibility of the involvement of this molecule. We looked at the biological responses of LIF-R–positive ARMS and ERMS cell lines to stimulation by exogenous LIF or OSM, such as phosphorylation of signaling proteins, cell proliferation, survival of rhabdomyosarcoma cells exposed to chemotherapy, adhesion, chemotaxis, chemoinvasion, and expression of matrix metalloproteinases (MMP).

Our findings provide evidence for first time that the LIF–LIF-R (cytokine–gp190 signaling receptor axis) regulates the metastatic behavior of rhabdomyosarcoma cells and their metastasis to the bone marrow and suggest that it could also contribute to their resistance to conventional methods of treatment.

Materials and Methods

Cell lines. We used human rhabdomyosarcoma cell lines (gift of Dr. Peter Houghton, St. Jude Children's Research Hospital, Memphis, TN) comprising ARMS lines (RH1, RH28, RH30, and CW9019) and ERMS lines

Requests for reprints: Mariusz Z. Ratajczak, Stem Cell Biology Program at James Graham Brown Cancer Center, University of Louisville, Delia Baxter Research Building, Room 118E, 580 South Preston Street, Louisville, KY 40202. Phone: 502-852-1788; Fax: 502-852-3032; E-mail: mzrata01@louisville.edu.

doi:10.1158/0008-5472.CAN-06-1021

(RH18, RD, and SMS-CTR), all established at St. Jude Hospital (Memphis, TN; ref. 5). The ERMS cell line, RD, was transfected with the *PAX3-FKHR* gene (gift of Dr. Frederic G. Barr; ref. 11).

Fluorescence-activated cell sorting analysis. The expression of gp190 protein, a common subunit for LIF-R, on various rhabdomyosarcoma cell lines and of both gp190 and CXCR4 on isolated subpopulations of the RH30 cell line was evaluated by fluorescence-activated cell sorting (FACS) as described previously (11, 14). The gp190 antigen was detected with anti-gp190 monoclonal antibody (mAb; Becton Dickinson PharMingen, San Diego, CA), clone 12D3, phycoerythrin conjugated, and CXCR4 was detected with mAb (Becton Dickinson PharMingen), clone 12G5, phycoerythrin conjugated. Samples stained with appropriate isotype controls (Becton Dickinson PharMingen) were examined in parallel.

Detection of LIF-R by Western blot. LIF-R was detected by protein immunoblotting (11) using rabbit anti–LIF-R antibody (clone C19; Santa Cruz Biotechnology, Santa Cruz, CA), with horseradish peroxidase (HRP)–conjugated goat anti-rabbit IgG (Santa Cruz Biotechnology) as secondary antibodies. Equal loading in the lanes was evaluated by stripping the blots and reprobing them with rabbit anti-AKT protein (New England Biolabs, Beverly, MA). The membranes were developed with an enhanced chemiluminescence (ECL) reagent (Amersham Life Sciences, Little Chalfont, United Kingdom), dried, and exposed to film (HyperFilm, Amersham Life Sciences).

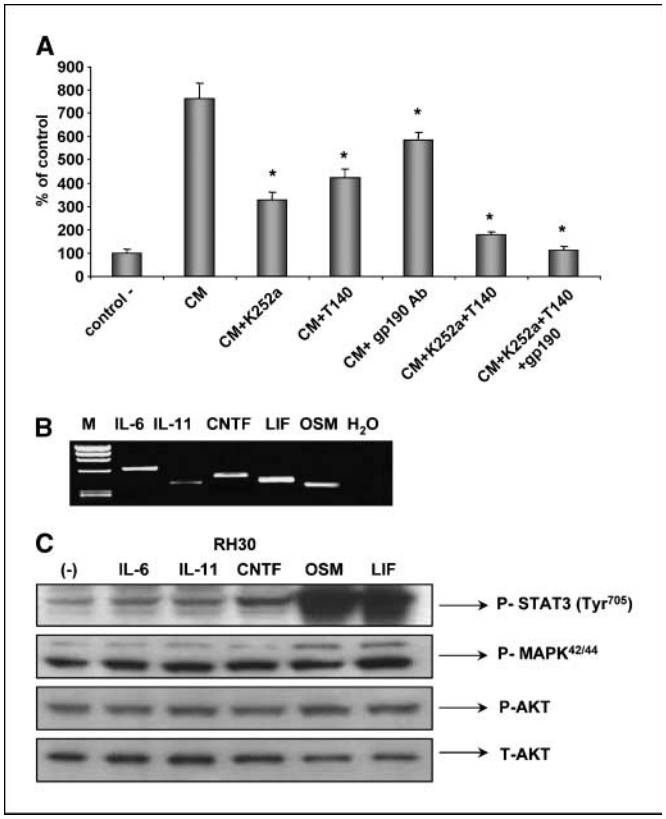

Figure 1. The gp130 signaling cytokines are expressed by bone marrow stroma and chemoattracted rhabdomyosarcoma cells. *A,* RH30 rhabdomyosarcoma cells respond by chemotaxis to conditioned medium (*CM*) harvested from bone marrow–derived fibroblasts. This chemotaxis is partially inhibited by c-met inhibitor (K252a), CXCR4 inhibitor (T140), and blocking antibodies against gp190 signaling protein. The most efficient inhibition was observed when all these inhibitors were used together. Data from four separate experiments are pooled together. *, $P < 0.0001$. *Bars*, SD. *B,* bone marrow–derived fibroblasts express mRNA for interleukin (IL)-6, IL-11, ciliary neurotrophic factor (CNTF), LIF, and OSM. The experiment was repeated twice with similar results. Representative study. *C,* analysis of phosphorylation of STAT3, MAPK p42/44, and AKT in the RH30 cell line stimulated by IL-6, IL-11, CNTF, OSM, and LIF (100 ng/mL for 5 min). The experiment was repeated thrice with similar results. Representative study.

Phosphorylation of intracellular pathway proteins. Rhabdomyosarcoma cell lines were kept in RPMI 1640 containing low levels of bovine serum albumin (BSA) (0.5%) to render them quiescent and then divided and stimulated with optimal doses of LIF (100 ng/mL) or OSM (100 ng/mL) for 5 min at 37°C before lysing for 10 min on ice in M-Per lysing buffer (Pierce, Rockford, IL) containing protease and phosphatase inhibitors (Sigma, Milwaukee, WI). Subsequently, the extracted proteins were separated on a 10% SDS-PAGE gel, and the fractionated proteins were transferred to a nitrocellulose membrane (Schleicher & Schuell, Keene, NH) as described previously (11, 14). Phosphorylation of the intracellular kinases, 44/42 mitogen-activated protein kinase (MAPK; Thr^{202}/Tyr^{204}), AKT (Ser^{473}), and signal transducers and activators of transcription 3 (STAT3; Tyr^{705}) proteins was detected using commercial mouse phospho-specific mAb (p44/42) or rabbit phospho-specific polyclonal antibodies for each of the remainder (all from New England Biolabs) with HRP-conjugated goat anti-mouse IgG or goat anti-rabbit IgG as secondary antibodies (Santa Cruz Biotechnology) as described (11, 14). Equal loading in the lanes was evaluated by stripping the blots and reprobing with appropriate mAbs: p42/44 anti-MAPK antibody clone 9102, anti-AKT antibody clone 9272, and anti-STAT3 (New England Biolabs). The membranes were developed with an ECL reagent, dried, and subsequently exposed to film (HyperFilm).

Transmembrane chemotaxis. The 8-μm pore polycarbonate membranes were covered with 50 μL of 0.5% gelatin. Cells were detached (with 0.5 mmol/L EDTA), washed in RPMI 1640, resuspended in RPMI 1640 with 0.5% BSA, and seeded at a density of 3×10^4 in 120 μL into the upper chambers of Transwell inserts (Costar Transwell, Corning Costar, Corning, NY). The lower chambers were filled with medium containing LIF (100 ng/mL) or OSM (100 ng/mL) or conditioned medium or 0.5% BSA RPMI 1640 (control). After 24 h, the inserts were removed from the Transwells, cells remaining in the upper chambers were scraped off with cotton wool, and cells that had transmigrated were stained by HEMA 3 (Protocol, Fisher Scientific, Pittsburgh, PA) and counted either on the lower side of the membranes or on the bottom of the Transwells.

Some of the directional migration experiments to conditioned medium harvested from bone marrow–derived fibroblasts were done using cells preincubated for 30 min at 37°C in the presence of 1 μmol/L T140-truncated polyphemusin analogue (a gift from Dr. Nobutaka Fujii, Kyoto University, Sakyo-Ku, Kyoto, Japan) and/or preincubated in the presence of 1 μmol/L c-met inhibitor, K-252a (Calbiochem-Novabiochem International, San Diego, CA), and/or 0.5 μg/mL anti-gp190 antibody (R&D Systems, Minneapolis, MN). conditioned medium from bone marrow–derived fibroblasts was obtained from cells cultured for 24 h in serum-free medium as described previously (11).

Adhesion of rhabdomyosarcoma cells to fibronectin, human umbilical vascular endothelial cell, or bone marrow stroma cells. Rhabdomyosarcoma cells were labeled with the fluorescent dye calcein-AM (2 μg/mL; Becton Dickinson BioCoat, Bedford, MA) in 37°C and 5% CO_2 and subsequently seeded (for 5 min) onto the 96-well plates covered with fibronectin, human umbilical vascular endothelial cells (HUVEC), or bone marrow stroma cells as described (11, 19). The cells were pretreated with LIF (100 ng/mL), OSM (100 ng/mL), or not (control or spontaneous adhesion of isolated subpopulations). Following incubation (at 37°C), the plates were washed thrice and cells that had adhered were counted using fluorescent inverted microscopy (Olympus America, Melville, NY).

Survival of rhabdomyosarcoma cells in Teflon wells. To prevent their adhesion, rhabdomyosarcoma cells were incubated for 6 h in Teflon wells with 100 ng/mL LIF or 100 ng/mL OSM or under control conditions (RPMI 1640 containing 0.5% BSA). Subsequently, cells were exposed for 24 h to etoposide (6 μmol/L), washed, and plated into new wells in 10% FCS RPMI 1640 and left for 3 days. The living cells were then stained by the fluorescent dye calcein-AM (2 μg/mL) and the number of living cells was determined by fluorescent inverted microscopy.

Isolation of mRNA and reverse transcription-PCR. For analysis of LIF and OSM mRNA, total mRNA was isolated from rhabdomyosarcoma cells with the RNeasy Mini kit (Qiagen, Inc., Valencia, CA), and mRNA was reverse transcribed with Taqman Reverse Transcription reagents (Applied Biosystems, Branchburg, NJ). The PCR was carried out with

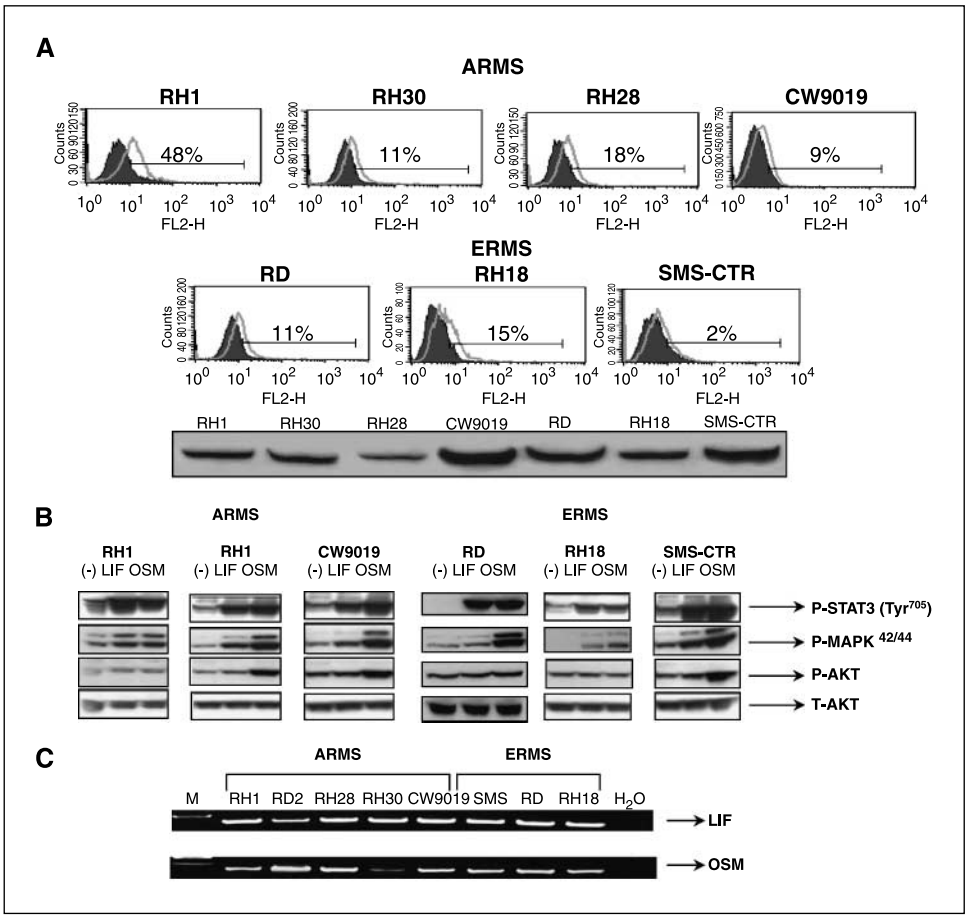

Figure 2. Human rhabdomyosarcoma cell lines express functional LIF-R. *A,* flow cytometry (*top*) and Western blot analysis (*bottom*) were done for gp190 on ARMS and ERMS cell lines. The experiments were repeated thrice (FACS) and twice (Western blot) with similar results. Representative studies. *B,* phosphorylation of STAT3, MAPK p42/44, and AKT in selected human rhabdomyosarcoma cell lines stimulated by LIF or OSM (100 ng/mL for 5 min). The experiment was repeated twice with similar results. Representative study. *C,* expression of mRNA for LIF and OSM was detected in human ARMS and ERMS cells by RT-PCR. The experiment was repeated twice on two different batches of cells with similar results. Representative study.

the LIF 5′ AAGGTCTTGGCGGCAGGAGTTGTG-3′ sense primer and the 5′-GATGTCGGCGGTGGCGTTGAG-3′ antisense primer and the OSM 5′-GGCCTGCCGGTCCTTCCCTCTC-3′ sense primer and the 5′-AGCGCCATTTGCACCACCTGTCC antisense primer. The predicted size of the reverse transcription-PCR (RT-PCR) product for LIF was 426 bp and for OSM was 415 bp. Amplified products (10 μL) were electrophoresed on a 1.5% agarose gel and transferred to a nylon filter.

Real-time RT-PCR. Quantitative assessment of LIF-R, CXCR4, and β-actin mRNA levels was done by real-time RT-PCR using an ABI Prism 7000 Sequence Detection System (ABI, Foster City, CA). Primers were designed with Primer Express software as follows: 3′-ATACGTAAATATCCATCATCTGTGCAA and 5′ GGAGCCTCTGCGACTCATTCA (LIF-R); 3′-GGGTTCCTTCATGGAGTCATAGCT and 5′-CGGTTACCATGGAGGGGATC (CXCR4); and 5′-CGGAACCGCTCATTGCC-3′ and 5′-ACCCACACTGTGCCCATCTA-3′ (β-actin). A 25-μL reaction mixture containing 12.5 μL SYBR Green PCR Master Mix and 10 ng cDNA template and primers was used. The threshold cycle (C_t; i.e., the cycle number at which the amount of amplified gene of interest reached a fixed threshold) was subsequently determined. Relative quantitation of LIF-R and CXCR4 mRNA expression was done with the comparative C_t method as described (17). The relative quantitation value of target, normalized to an endogenous control *β-actin* (housekeeping) gene and relative to a calibrator, is expressed as $2^{-\Delta\Delta Ct}$ (fold difference), where ΔC_t = [C_t of target genes (LIF-R and CXCR4)] − [C_t of endogenous control gene (β-actin)] and $\Delta\Delta C_t$ = (ΔC_t of samples for target gene) − (ΔC_t of calibrator for the target gene).

Fluorescent staining of F-actin, focal adhesion kinase, and paxillin. To visualize the actin cytoskeleton, cells were cultured for 12 h on glass coverslips in RPMI 1640 supplemented with 10% fetal bovine serum (FBS) and after that the medium was removed and the cells were washed by PBS and incubated in RPMI 1640 containing low levels of BSA (0.5%) to render them quiescent. Next, the cells were stimulated by LIF or OSM (100 ng/mL) and fixed in 3.7% paraformaldehyde/Ca- and Mg-free PBS for 20 min, permeabilized by 0.1% Triton X-100 in PBS for 1 min at room temperature, and stained for 1 h with Alexa 488-phalloidin (Molecular Probes, Eugene, OR) to detect F-actin, with monoclonal mouse anti-paxillin antibody (Upstate Biotechnology, Lake Placid, NY) and goat anti-mouse Alexa 488 to detect paxillin and monoclonal mouse anti–focal adhesion kinase (FAK) antibody (Upstate Biotechnology) and goat anti-mouse Alexa 594 (Molecular Probes) to detect FAK. Specimens were counterstained with 0.5 μg/mL *bis*-benzimide (Hoechst) to visualize the nuclei. After being washed, the cells were embedded in Vectashield mounting medium (Vector Laboratories, Peterborough, United Kingdom) and analyzed with a BX51 fluorescence microscope (Olympus America) equipped with a charge-coupled device camera (Olympus America). Each staining was repeated thrice.

Rho activation assay. Rho activity was measured in a rhabdomyosarcoma cell line using the Rho activation assay kit according to the manufacturer protocol (Upstate Biotechnology). Before the assay, cells were kept in RPMI 1640 containing low levels (0.5%) of BSA to render them quiescent and then aliquoted and stimulated by optimal doses of LIF for 1, 3, and 5 min. Cell lysates were precleared by centrifugation (14,000 rpm for 5 min at 4°C) and incubated with Rhotekin binding domain-tagged agarose (10 μg) by gentle rocking at 4°C for 1 h. The GTP-bound form of Rho was detected through Western blot analysis using monoclonal anti-Rho antibody (clone 55; Upstate Biotechnology).

Cell proliferation. Cells were plated in 24-well culture plates at an initial density of 10^4 cells/cm^2 in the presence or absence of LIF (100 ng/mL) or OSM (100 ng/mL) and counted at 12, 24, 36, 48, and 60 h after culture initiation (in some experiments also at 72 h) as described (11).

Knockdown of LIF-R with small interfering RNA. We purchased predesigned small interfering RNA (siRNA) duplexes for LIF-R (Genbank accession no. NM_002310): LIF-R 1 sense and [r(AGACCAUUAUCAACUCCUA)dTdT] and scramble control sense (UUCUCCGAACGUGUCAC-

GUdTdT; Qiagen). The RH30 cell line was cultured for 24 h before transfection in Opti-MEM–reduced serum medium (Life Technologies, Invitrogen Corp., Carlsbad, CA). The siRNAs were transfected into RH30 cells at a final concentration of 100 nmol/L using LipofectAMINE 2000 (Invitrogen, Carlsbad, CA). To determine the efficiency of siRNA, at 48 h post-transfection, the transfected cells were collected to measure the expression of LIF-R at the mRNA level by real-time quantitative PCR (RQ PCR) and the protein level by Western blot as described above.

Transplants of rhabdomyosarcoma cells into immunodeficient mice. To evaluate the *in vivo* metastatic behavior of three populations of RH30 cell lines (RH30, RH30 -L, and RH30-S), the cells were injected i.v. (8×10^6 per mouse) into immunodeficient severe combined immunodeficient (SCID)-Beige inbred mice. In some experiments, mice were transplanted with RH30 cells exposed to siRNA against LIF-R, cells exposed to scramble siRNA, or nonexposed cells. Marrows and livers were removed 48 h after injection of these cells and the presence of rhabdomyosarcoma cells (i.e., murine-human chimerism) was evaluated as the difference in the level of human α-satellite. DNA was amplified in the extracts isolated from the bone marrow–derived and the liver-derived cells, using real-time PCR. Briefly, DNA was isolated using the QIAamp DNA Mini kit (Qiagen). Detection of human α-satellite and murine β-actin DNA levels was done using real-time PCR and an ABI Prism 7000 Sequence Detection System. A 25-μL reaction mixture containing 12.5 μL SYBR Green PCR Master Mix; 300 ng DNA template; 5′-GGGATAATTTCAGCTGACTAAACAG-3′, 5′-TTTCGTTTAGTTAGGTGCAGTTATC-3′, and 5′-AAACGTCCACTTGCAGATTCTAG-3′ primers for the α-satellite; and 5′-GGATGCAGAAGGAGATCACTG-3′ forward and 5′-CGATCCACACGGAGTACTTG-3′ reverse primers for the β-actin. C_t was determined as before. The number of human cells present in the murine organs (degree of chimerism) was calculated from the standard curve obtained by mixing different numbers of human cells with a constant number of murine cells.

In some of the experiments, RH30-L and RH30 cells (5×10^6 per mouse) were inoculated into the hind limb muscles of immunodeficient SCID-Beige inbred mice. Six weeks later, the mice were sacrificed for evaluation of rhabdomyosarcoma cells present in bone marrow, liver, and lungs. Detection of human cells was done as described above.

Statistical analysis. All results are presented as mean ± SE. Statistical analysis of the data was done using the nonparametric Mann-Whitney test, with $P < 0.05$ considered significant.

Results

LIF and OSM are expressed in bone marrow–derived stroma cells and chemoattracted rhabdomyosarcoma cells. The metastasis of rhabdomyosarcoma cells to the bone marrow is directed by SDF-1 (11) and HGF (12–14) and we show here that the chemotactic responses of RH30 cells to bone marrow–derived

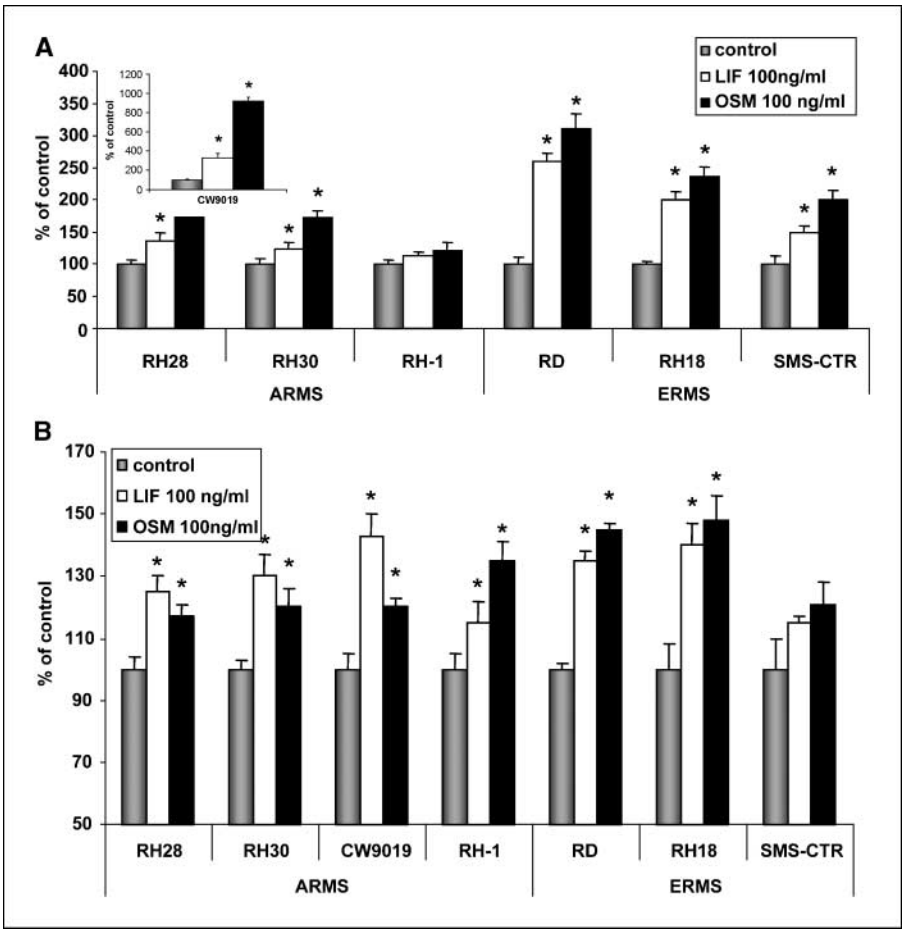

Figure 3. LIF and OSM increase chemotaxis and adhesiveness of rhabdomyosarcoma cells. *A,* chemotaxis of rhabdomyosarcoma cells across Transwell membranes to LIF or OSM gradient. ARMS cell lines RH28, RH30, RH-1, and CW9019 and ERMS cell lines RD, SMS-CTR, and RH18 were tested for their chemotactic responsiveness to LIF or OSM gradient. *Gray columns,* chemotaxis to control medium (no LIF in lower chamber); *white columns,* chemotaxis to LIF (100 ng/mL); *black columns,* chemotaxis to OSM (100 ng/mL). Data from four separate experiments are pooled together. *, $P < 0.0001$. *B* to *D,* LIF and OSM increase adhesiveness of rhabdomyosarcoma cells. Adhesion of human rhabdomyosarcoma cells to fibronectin (*B*), HUVEC (*C*), and bone marrow–derived stroma cells (*D*) was tested in rhabdomyosarcoma cells not stimulated (control; *gray columns*) or stimulated with LIF (*white columns*) or OSM (*black columns*) was tested. Data from four separate experiments are pooled together. *, $P < 0.0001$. *Bars*, SD.

conditioned medium could be significantly but not completely inhibited by blocking of the CXCR4 and c-met receptors on rhabdomyosarcoma cells or the gp190 protein (Fig. 1*A*). However, when the CXCR4 antagonist (T140), the c-met blocking agent (K252a), and the gp190 blocking antibody were used together, the chemotaxis of the highly metastatic ARMS cell line RH30 was inhibited completely (Fig. 1*A*).

To learn more of the role of gp130 signaling cytokines in rhabdomyosarcoma metastasis, we evaluated their expression in bone marrow–derived fibroblasts and showed that they express several gp130 signaling cytokines (Fig. 1*B*) that could be potential chemotactic factors for rhabdomyosarcoma cells. Because two gp130 signaling cytokines, LIF and OSM, are involved in the development of skeletal muscles (18), we asked whether these factors play a role in directing metastases of rhabdomyosarcoma cells to bone marrow. We found that of the five gp130 signaling cytokines tested, only LIF and OSM efficiently stimulated phosphorylation of STAT3 and MAPK p42/44 in RH30 cells (Fig. 1*C*); therefore, we concentrated our attention on these two cytokines in further experiments.

Rhabdomyosarcoma cell lines express functional LIF-R. First, we phenotyped several human rhabdomyosarcoma cell lines by FACS for expression of LIF-R and found that all four ARMS (RH1, RH28, RH30, and CW9019) and all three ERMS (RD, RH18, and SMS-CTR) cell lines expressed mRNA for LIF-R (data not shown) and for the gp190 protein, a common subunit for LIF-R and OSM receptor (OSM-R; Fig. 2*A*). Expression of gp190 protein was also confirmed by Western blot (Fig. 2*A*). In our previous studies, we observed that PAX3-FKHR overexpression in the ERMS cell line RD correlated with up-regulation of expression of CXCR4 (11) and c-met (14). In the current study, however, expression of mRNA for LIF-R or of gp190 on the cell surface was not affected after RD ERMS cells were stable transfected with the PAX3-FKHR expression vector (data not shown).

Next, we found that stimulation of various rhabdomyosarcoma cell lines by LIF or OSM, like the RH30 cell line (Fig. 1*C*), induced the phosphorylation of STAT3 in all these cell lines (Fig. 2*B*). In addition, MAPK p42/44 was phosphorylated in all and AKT was phosphorylated in most of the cell lines tested (Fig. 2*B*).

LIF and OSM do not influence proliferation of rhabdomyosarcoma cell lines but may increase their survival. Next, we examined the ARMS (RH1, RH28, RH30, and CW9019) and the ERMS (RD, RH18, and SMS-CTR) cell lines to determine whether LIF or OSM affects their proliferation. We stimulated them with LIF

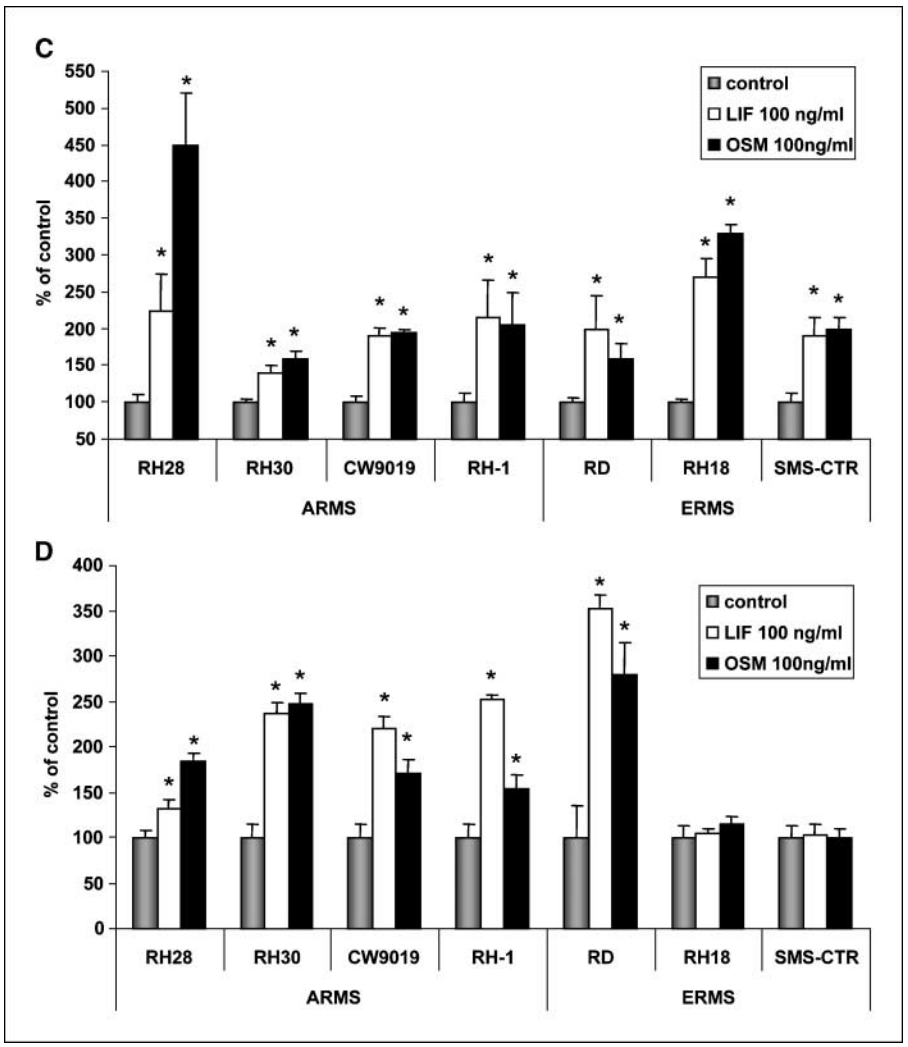

Figure 3 *Continued.*

or OSM or neither (control) in serum-free conditions or in medium supplemented with 0.5% BSA and found that the rhabdomyosarcoma cell lines proliferated intensively during 72 h under all types of conditions. The kinetics of proliferation were similar and not affected by the presence of LIF or OSM in the culture, even when the cells were cultured for up to 7 days (data not shown).

Because the biology of various tumors may be regulated by autocrine/paracrine axes (20), we next tested whether these rhabdomyosarcoma cells express LIF or OSM. We found that all cell lines investigated in this study expressed mRNA for these factors (Fig. 2*C*). However, blocking the putative LIF/OSM-gp190–coupled LIF-R and OSM-R autocrine regulatory axis by adding anti-gp190 blocking mAb or siRNA did not affect the proliferation kinetics of these cell lines (data not shown).

Next, we evaluated whether signaling through a gp190 receptor enhances the survival of rhabdomyosarcoma cells. To address this issue, we incubated two ARMS cell lines (RH30 and CW9019) in Teflon wells, which prevents their adhesion, for 6 h with 100 ng/mL LIF or OSM. Subsequently, both ARMS cell lines were exposed to etoposide (6 μmol/L). After 24 h of incubation, the cells were washed to remove the etoposide and plated in new wells in 10% FBS RPMI 1640 for 3 days. After this, the surviving cells were scored using the 0.4% trypan blue exclusion assay. We found that preincubation of rhabdomyosarcoma cells with LIF or OSM (100 ng/mL) significantly increased their survival and subsequent expansion and that these cells were better able to proliferate after removal from etoposide (6 μm)–containing medium, suggesting that LIF and OSM may protect rhabdomyosarcoma cells from chemotherapy. Accordingly, ×5 and ×2 more cells were observed in cultures initiated by RH30 and CW9019 cells that were coincubated with LIF or OSM during exposure to etoposide.

Of note, in control experiments, LIF or OSM did not affect survival/proliferation of rhabdomyosarcoma cells incubated for 6 h in Teflon dishes, suggesting that the biological effect of these factors correlates with cell adhesiveness.

LIF or OSM increases migration across fibronectin-covered Transwell membranes. Next, we investigated the directed migration of rhabdomyosarcoma cells through membranes covered with fibronectin. We found that LIF and OSM significantly increased the chemotactic activity of the ARMS cell lines RH28, RH30, and CW9019 and the ERMS cell lines RH18, SMS-CTR, and RD (Fig. 3*A*). This correlated with phosphorylation of MAPK p42/44 (Figs. 1*C* and 2*B*), confirming an important role for this pathway in regulating the motility of rhabdomyosarcoma cells (11, 14).

LIF or OSM increase adhesion of rhabdomyosarcoma cells. Cell adhesion is an important step in rhabdomyosarcoma metastasis and we found that both LIF and OSM affected the adhesion of the rhabdomyosarcoma cell lines tested to fibronectin, HUVEC, and bone marrow–derived fibroblasts (Fig. 3*B–D*). However, when we investigated using FACS analysis whether LIF or OSM regulates expression/activation of integrins on human rhabdomyosarcoma, we did not find any change in the level of expression of VLA-4, VLA-5, platelet/endothelial cell adhesion molecule 1, or intercellular adhesion molecule 1 on rhabdomyosarcoma cells after incubation with LIF or OSM for 24 h (data not shown).

LIF stimulates stress fiber formation, colocalization of FAK and paxillin in focal contacts, and Rho activation. Next, we focused on molecular mechanisms related to the LIF-mediated adhesion of rhabdomyosarcoma cells. As a model, we used the ARMS cell line CW9019 that shows enhanced migration through fibronectin-covered membranes and strong adhesion to fibronectin, HUVEC, and bone marrow–derived stroma cells (Fig. 3). First, using immunofluorescence staining, we observed that in serum-starved rhabdomyosarcoma cells, LIF stimulates the formation of strong F-actin bundles, which colocalized with FAK in the filopodia (Fig. 4*A*). Next, we investigated whether LIF also colocalizes paxillin and FAK in rhabdomyosarcoma cells and found that both colocalized in focal adhesion complexes in the filopodia after LIF stimulation (Fig. 4*B*). At the same time, we found by Western blotting that Rho becomes activated in LIF-stimulated cells (Fig. 4*C*).

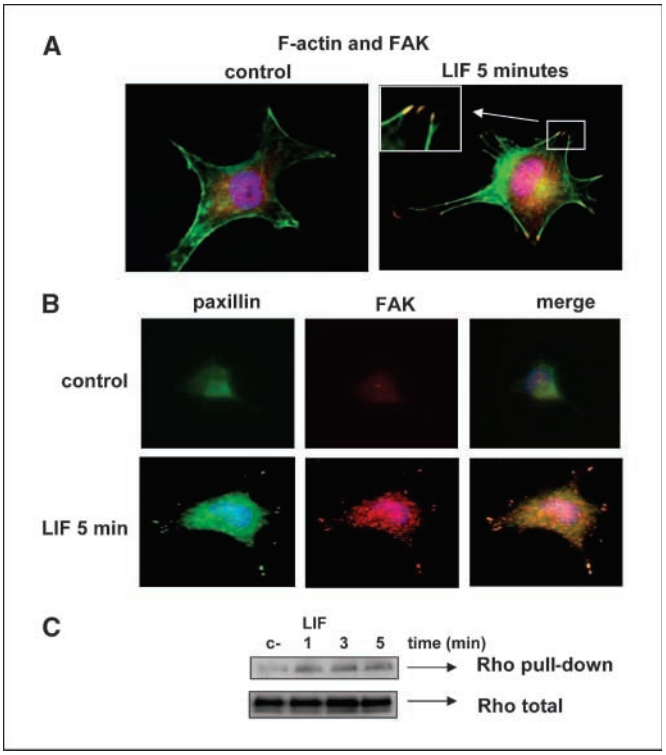

Figure 4. LIF induces F-actin formation and colocalization of FAK, F-actin, and paxillin in rhabdomyosarcoma cells. *A,* F-actin is stained with Alexa 488-phalloidin and FAK with anti-FAK antibody and goat anti-mouse Alexa 594. Specimens were counterstained with 0.5 μg/mL bis-benzimide (Hoechst) to visualize the nuclei. *Inset,* colocalization of F-actin and FAK, high power (*yellow*). *B,* paxillin was stained with anti-paxillin antibody and goat anti-mouse Alexa 488 and FAK with monoclonal mouse anti-FAK antibody and goat anti-mouse Alexa 594. Specimens were counterstained with 0.5 μg/mL bis-benzimide (Hoechst) to visualize the nuclei. Cells in (*A*) and (*B*) were analyzed with a fluorescence microscope equipped with a charge-coupled device camera. Each staining was repeated thrice on different cell samples. Representative data. *C,* Rho activity was measured in a rhabdomyosarcoma cell line using the Rho activation assay kit. Cells were stimulated by optimal doses of LIF for 1, 3, and 5 min, lysed, and subsequently incubated with the Rhotekin binding domain tagged. The GTP-bound form of Rho was detected with Western blot analysis using monoclonal anti-Rho antibody. The experiment was repeated thrice with similar results. Representative result.

In control experiments, LIF did not affect translocation of FAK or paxillin to focal adhesion complexes in the ERMS cell line SMS-CTR, which did not respond by increased adhesion to LIF or OSM stimulation (data not shown).

LIF as a regulator of rhabdomyosarcoma cell metastasis. Chemotaxis of the ARMS cell line RH30 to conditioned medium harvested from bone marrow–derived fibroblasts was inhibited after perturbation of signaling from CXCR4 or LIF-R (Fig. 1*B*). To better define the role of the LIF–LIF-R axis versus the SDF-1–CXCR4 axis in the metastasis of rhabdomyosarcoma cells, we did repetitive chemotaxis to LIF or SDF-1 to select RH30 cells that

responded robustly to one or the other chemoattractant, which we called RH30-L and RH30-S cells, respectively. We found that the RH30-L cells were bigger, more flattened, and adhered better to plastic than the RH30-S cells. However, the most striking difference was that RH30-L cells proliferated better *in vitro* in standard culture medium compared not only to RH30-S but also to the parental RH30 cells (data not shown).

Using real-time RT-PCR, we found that mRNA for LIF-R and CXCR4 is up-regulated in RH30-L and RH30-S cells, respectively, compared with parental RH30 cells (Fig. 5*A*), corresponding with changes at the protein level as evaluated by FACS analysis (Fig. 5*B*). At the same time, expression of LIF-R was down-regulated in RH30-S and CXCR4 in RH30-L cells, at both the mRNA and protein levels (Fig. 5*A* and *B*).

To investigate further the roles of LIF–LIF-R and SDF-1–CXCR4 axes in the metastasis of RH30 cells, we tested parental RH30, RH30-L, and RH30-S cells for various properties related to their metastatic behavior. First, we noticed in adhesion assays that RH30-L cells show much higher spontaneous adhesion to bone marrow–derived fibroblasts than parental RH30 and RH30-S cells (Fig. 5*C*). Next, when we tested their chemotactic responsiveness to conditioned medium derived from bone marrow stroma fibroblasts, we found that in this assay, RH30-L cells show much lower chemotaxis to bone marrow stroma-derived conditioned medium compared with parental RH30 and selected RH30-S cells (Fig. 5*D*).

The role of the LIF–LIF-R axis in the metastasis of rhabdomyosarcoma cells *in vivo*. To learn more about the role of the LIF–LIF-R axis in the metastasis of rhabdomyosarcoma cells, we injected RH30, RH30-L, and RH30-S cells i.v. into immunodeficient SCID-Beige inbred mice and 48 h later evaluated the seeding of these human cells into murine bone marrow and liver. To estimate the number of human cells that seed to bone marrow and liver in SCID-Beige immunodeficient mice, we isolated DNA and using real-time RT-PCR amplified human α-satellite sequences and murine β-actin. We found that RH30-L cells showed four to five times higher seeding efficiency into the bone marrow and liver of immunodeficient SCID-Beige mice than parental RH30 and RH30-S cells (Fig. 6*A*).

Next, RH30 or RH30-L cells (5×10^6 per mouse) were injected i.m. into the hind limb. Six weeks later, we evaluated the number of human rhabdomyosarcoma cells present in the bone marrow, lung, and livers of animals inoculated with rhabdomyosarcoma cells. We found a significant increase in number of rhabdomyosarcoma cells in the bone marrow and lungs of mice injected with RH30-L cells (Fig. 6*B*).

Finally, we down-regulated the expression of LIF-R in RH30 cells using the siRNA strategy (Fig. 6*C, inset*). Next, RH30 cells

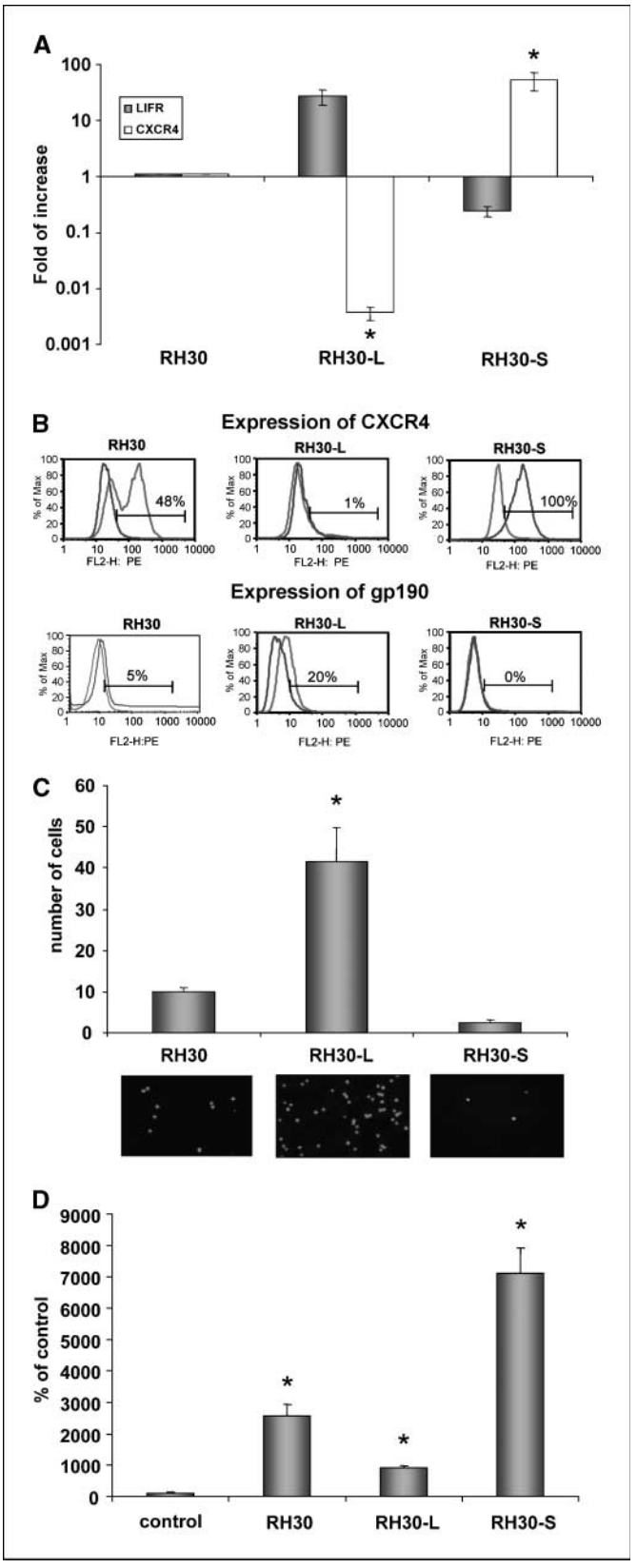

Figure 5. Two populations of the RH30 cell line isolated by repetitive chemotactic gradient to LIF or SDF-1. RH30 cells were chemoattracted to LIF or SDF-1 in chemotaxis assays. Cells that responded to chemoattractants were separated and cultured. The procedure was repeated thrice to obtain RH30 cells that highly expressed LIF-R but not CXCR4 and vice versa for cells that highly expressed CXCR4 but not LIF-R. Expression of the LIF-R and CXCR4 receptors was evaluated in RH30 parental and RH30-L and RH30-S cells by real-time RT-PCR (*A*) or by FACS (*B*). Real-time PCR data are pooled together from three independent experiments. *, $P < 0.000001$. FACS analysis was repeated thrice with similar results. Representative result. *C* to *D,* RH30-L cells show greater adhesion *in vitro* and metastatic potential *in vivo*. *C,* spontaneous adhesion of RH30 parental cells or LIF- or SDF-1–selected cells to bone marrow–derived stroma cells. Calcein-AM–labeled RH30 cells were layered over bone marrow stroma cells. After 10 min, the nonadherent cells were removed and the number of adherent cells was counted using an inverted fluorescent microscope. Data are pooled together from three independent experiments. *, $P < 0.0001$. *D,* chemotaxis of RH30 parental cells or LIF- or SDF-1–selected cells to bone marrow fibroblast-derived conditioned medium. *, $P < 0.0001$. *Bars,* SD.

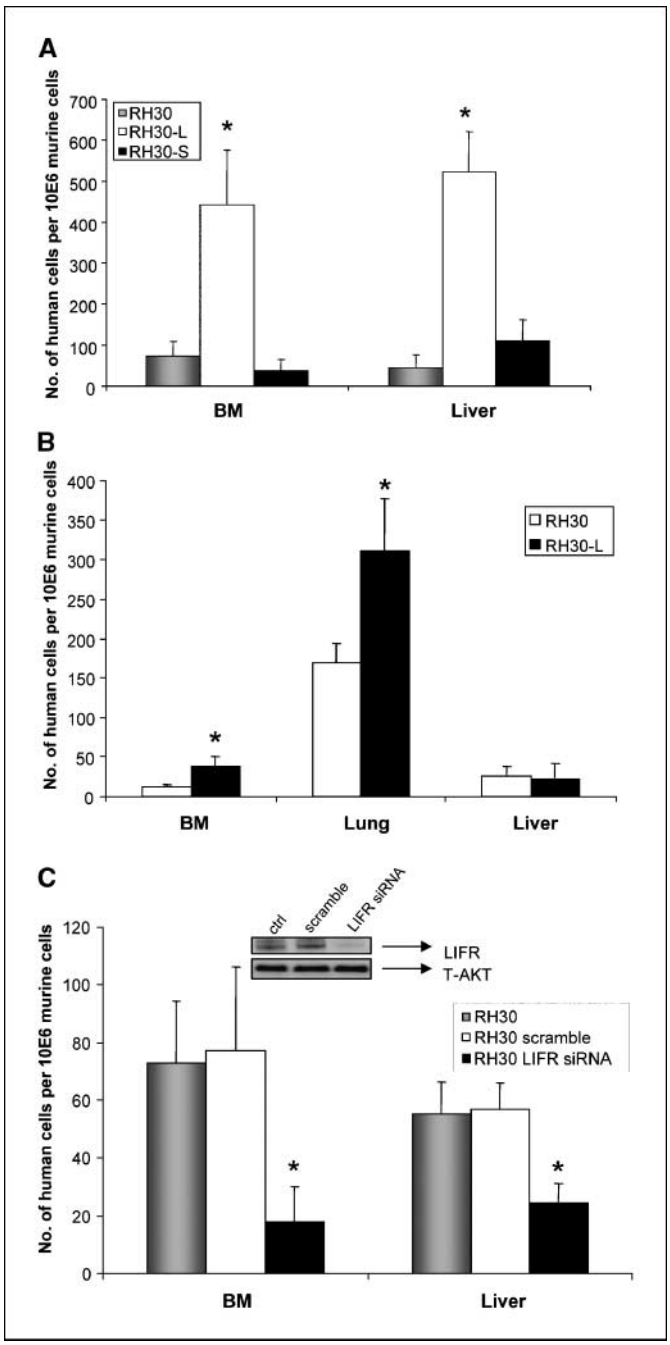

Figure 6. The role of the LIF–LIF-R axis in *in vivo* metastasis of rhabdomyosarcoma cells. *A,* RH30 parental cells or LIF- or SDF-1–selected cells were injected i.v. into SCID-Beige mice and organs were harvested after 48 h for DNA isolation. The number of human cells was estimated by real-time RT-PCR per 10^6 murine cells. Real-time PCR data are pooled together from three independent experiments (five mice per experiment). *, $P < 0.0001$. *B,* RH30 parental cells or LIF–selected cells (RH30-L) were injected (5×10^6 per mouse) into the hind limb muscles of SCID-Beige mice. Six weeks later, bone marrow, liver, and lungs were harvested for DNA isolation. The number of human cells was estimated by real-time RT-PCR per 10^6 murine cells. Real-time PCR data are pooled together from two independent experiments (eight mice per experiment). *, $P < 0.0001$. *C,* RH30 parental cells were exposed to LIF-R siRNA. Cells with down-regulated by siRNA LIF-R expression (*inset*) and controls (untreated cells and cells exposed to scramble siRNA) were injected i.v. into SCID-Beige mice and the organs were harvested after 48 h for DNA isolation. The number of human cells was estimated by real-time RT-PCR per 10^6 murine cells. Real-time PCR data are pooled together from two independent experiments (eight mice per experiment). *, $P < 0.0001$. *Bars,* SD.

with down-regulated LIF-R expression or unmanipulated RH30 cells or cells exposed to scramble siRNA were injected i.v. into immunodeficient mice. The number of human rhabdomyosarcoma cells in murine bone marrow and liver was evaluated by RQ-PCR 48 h later, based on the presence of human DNA in bone marrow and liver DNA extracts. We found that down-regulation of LIF-R on RH30 cells significantly decreases the seeding efficiency of rhabdomyosarcoma cells into bone marrow and liver (Fig. 6*C*).

Discussion

In children and adolescents diagnosed with rhabdomyosarcoma, the involvement of bone marrow is a poor prognostic sign and represents a continuing challenge to current treatment modalities (2, 3, 21). There is thus a need for more effective therapies, and elucidating the mechanisms that control the metastasis of rhabdomyosarcoma cells could be a means to achieve this.

Both the SDF-1–CXCR4 and HGF/SF–c-met axes have been implicated in the metastasis of several solid tumors (22–31) and we have reported that rhabdomyosarcoma cells could be chemoattracted to the bone marrow by SDF-1 and HGF (11, 14). However, as we show here, inhibition of both axes did not completely inhibit the chemotaxis of rhabdomyosarcoma cells to conditioned medium harvested from bone marrow–derived fibroblasts, suggesting the involvement of other chemoattractants.

Because LIF plays a pivotal role in muscle regeneration (15–18), we hypothesized that LIF and OSM, which activate similar receptors, could be involved in the metastasis of rhabdomyosarcoma. To test this hypothesis, we evaluated the effect of anti-LIF-R antibodies that were added to the cocktail of CXCR4 and c-met inhibitors to see whether such a combination could inhibit migration of the highly metastatic ARMS cell line RH30. We provide the first evidence that blockade of gp190 inhibits the chemotaxis of solid tumor cells, suggesting direct involvement of LIF in the migration of rhabdomyosarcoma cells. The fact that LIF, like SDF-1 or HGF, is a morphogenic factor in organogenesis supports this observation. Furthermore, LIF may also be involved in the chemoattraction of circulating stem cells to damaged heart (17) or brain (32) as we recently show. Thus, LIF, initially thought to act as a hematopoietic cytokine (18), in fact displays various pleiotropic effects.

To elucidate in more detail the biological effects of LIF/OSM in rhabdomyosarcoma, we selected rhabdomyosarcoma cell lines that respond to stimulation by LIF by phosphorylation of MAPK p42/44 or STAT3 and tested whether these factors increase rhabdomyosarcoma cell proliferation. However, despite the fact that these signal transduction pathways are involved in regulating cell proliferation (33), we did not find that LIF had any effect on the proliferation of rhabdomyosarcoma cell lines. This is in striking contrast to normal skeletal muscle cells where LIF has been reported to act as a proliferative factor (33).

Next, we examined events directly related to cell metastatic/invasive behavior, such as resistance to chemotherapy, chemotaxis, adhesion, and production of MMPs. First, we found that LIF increases the survival of rhabdomyosarcoma cell lines during exposure to etoposide, a cytostatic commonly used to treat this tumor. Thus, LIF alone, or in combination with other factors, may stimulate the survival of metastasizing cells and make them more resistant to chemotherapy. We reported a similar effect for HGF (14) but not for SDF-1 (11). Because we have shown that LIF did

not enhance the survival of rhabdomyosarcoma cells when they are cultured in Teflon dishes (which prevents adhesion), we postulate that the prosurvival effect of LIF is closely related to the adhesive status of these cells. Thus, by increasing adhesion LIF indirectly increases the resistance of rhabdomyosarcoma cells to apoptosis. Hence, we suggest that targeting the LIF–LIF-R axis may be of therapeutic importance not only for controlling the metastatic behavior of rhabdomyosarcoma cells but also for improving the clinical outcome of chemotherapy. The molecular mechanism for this resistance, however, requires further study and is currently under investigation in our laboratory.

Furthermore, LIF strongly enhances adhesion of rhabdomyosarcoma cells to fibronectin, endothelial cells, and bone marrow–derived fibroblasts and stimulates stress fiber formation and at the molecular level colocalization of FAK and paxillin in focal contacts and activation of small GTPase Rho. It is well known that colocalization of FAK and paxillin in focal contacts is crucial for cell adhesion (34–36). Interestingly, LIF, SDF-1, and HGF did not affect expression of adhesion molecules on rhabdomyosarcoma cells.

In our previous studies, we observed that transcripts for MMP-2 and MMP-9 as well as membrane type-1 MMP and tissue inhibitor of metalloproteinase (TIMP)-2 were detectable in all the rhabdomyosarcoma cell lines tested (11, 14). Although LIF and OSM are chemoattractants for rhabdomyosarcoma cells, in contrast to SDF-1 (11) and HGF (14), we found that stimulation with LIF does not influence expression of MMPs or TIMPs, either at the mRNA (real-time RT-PCR) or protein (zymography and reverse zymography) levels in any of the rhabdomyosarcoma lines tested (data not shown). Thus, the effect of LIF in metastasis is not directly linked to modulation of the expression/secretion of MMPs.

Our previous and current data also show that metastasis of rhabdomyosarcoma is regulated by several prometastatic axes, such SDF-1–CXCR4, HGF-SF–c-met, and LIF–LIF-R; thus, strategies aimed on inhibition of only one of these axes may be not sufficient to prevent the spread of rhabdomyosarcoma cells. To compare the role of the LIF–LIF-R axis with that of SDF-1–CXCR4 axis in directing the metastasis of rhabdomyosarcoma cells, we obtained (by repetitive chemotactic isolation) two different populations of the highly metastatic RH30 cells. We observed that the RH30 cells selected by chemotaxis to LIF significantly enhanced spontaneous adhesion to bone marrow–derived fibroblasts in contrast to those selected by SDF-1 and even to the parental cell line. This increased adhesiveness corresponded with decreased motility of these cells to medium conditioned by the bone marrow stroma. Furthermore, in *in vivo* metastasis studies using LIF- and SDF-1–selected RH30 cells, the LIF-selected cells had much higher seeding efficiency to liver and bone marrow, implying that adhesion was a crucial component of their metastatic behavior. Similarly, mice inoculated i.m. with RH30-L cells had more rhabdomyosarcoma cells in the bone marrow and lung after 6 weeks compared with parental RH-30 cells. The metastatic potential of RH30 cells *in vivo* was inhibited by siRNA against LIF-R. It is likely that cells displaying increased motility tend to become "homeless" and ultimately undergo apoptosis, a notion, however, that requires further study.

As stated above, the alveolar type of rhabdomyosarcoma is more metastatic than the embryonal, and in our previous work, we hypothesized that increased expression of the CXCR4 and c-met receptors on ARMS cells could be modulated by the *PAX3-FKHR* fusion gene (12, 13, 37). In fact, the CXCR4 and c-met promoter contain several PAX binding sites and it has been reported that PAX3 modulates expression of the c-met receptor during limb development (37). Moreover, microarray analysis identified c-met as a PAX3 downstream target gene (12). In this study, we did not find a correlation between rhabdomyosarcoma type and LIF-R expression. Overexpression of the *PAX3-FKHR* fusion gene in the ERMS cell lines led to up-regulation of CXCR4 (11) and c-met (14) but did not affect expression of LIF-R. This suggests that LIF-R, in contrast to CXCR4 (11) and c-met (14), is not regulated by the *PAX3-FKHR* or *PAX7-FKHR* fusion genes. It also does not correlate with rhabdomyosarcoma type.

In conclusion, we present evidence for the first time that the LIF–LIF-R axis may direct metastasis and enhance the invasive potential of solid tumors (rhabdomyosarcoma). Hence, molecular targeting of LIF or LIF-R (e.g., as we show here using the siRNA strategy) has potential as a new antimetastatic strategy to improve therapeutic outcome for patients suffering from sarcomas. Molecular strategies aimed at inhibiting the LIF–LIF-R axis and the SDF-1–CXCR4 axis, for example, by the use of small-molecule inhibitors, could lead to the development of new antimetastatic therapies that could complement conventional radiotherapy or chemotherapy in preventing the dissemination of rhabdomyosarcoma cells into the bone marrow and lymph nodes.

Acknowledgments

Received 3/17/2006; revised 11/1/2006; accepted 12/15/2006.

Grant support: NIH grant R01 CA106281-01 grant (M.Z. Ratajczak), KBN grant 2POSA 00429 to MZR, and partially by "V Foundation".

The costs of publication of this article were defrayed in part by the payment of page charges. This article must therefore be hereby marked *advertisement* in accordance with 18 U.S.C. Section 1734 solely to indicate this fact.

References

1. Sharp R, Recio JA, Jhappan C, et al. Synergism between INK4a/ARF inactivation and aberrant HGF signaling in rhabdomyosarcomagenesis. Nat Med 2002; 11:1276–80.
2. Ruymann FB, Newton WA, Ragab AH, Donaldson MH, Foulkes M. Bone marrow metastases at diagnosis in children and adolescents with rhabdomyosarcoma. Cancer 1984;53:368–73.
3. Sandberg AA, Stone JF, Czarnecki L, Cohen JD. Hematologic masquerade of rhabdomyosarcoma. Am J Hematol 2001;68:51–7.
4. Barr FG, Galili N, Holick J, Biegel JA, Rovera G, Emanuel BS. Rearrangement of the PAX3 paired box gene in the paediatric solid tumour alveolar rhabdomyosarcoma. Nat Genet 1993;3:113–7.
5. Hazelton BJ, Houghton JA, Parham DM, et al. Characterization of cell lines derived from xenografts of childhood rhabdomyosarcoma. Cancer Res 1987;47: 4501–7.
6. Davis RJ, Barr FG. Fusion genes resulting from alternative chromosomal translocations are overexpressed by gene-specific mechanisms in alveolar rhabdomyosarcoma. Proc Natl Acad Sci U S A 1997;94:8047–51.
7. Davis RJ, D'Cruz CM, Lovell MA, Biegel JA, Barr FG. Fusion of PAX7 to FKHR by the variant t(1;13)(p36;q14) translocation in alveolar rhabdomyosarcoma. Cancer Res 1994;54:2869–72.
8. Collins MH, Zhao H, Womer RB, Barr FG. Proliferative and apoptotic differences between alveolar rhabdomyosarcoma subtypes: a comparative study of tumors containing PAX3-FKHR gene fusions. Med Pediatr Oncol 2000;37:83–9.
9. Bennicelli JL, Advani S, Schafer BW, Barr FG. PAX3 and PAX7 exhibit conserved *cis*-acting transcription repression domains and utilize a common gain of function mechanism in alveolar rhabdomyosarcoma. Oncogene 1999;18:4348–56.
10. Kelly KM, Womer RB, Barr F. 3-FKHR and PAX7-FKHR fusions in rhabdomyosarcoma. J Pediatr Hematol Oncol 1998;20:517–8.
11. Libura J, Drukala J, Majka M, et al. CXCR4-SDF-1 signaling is active in rhabdomyosarcoma cells and regulates locomotion, chemotaxis, and adhesion. Blood 2002;100:2597–606.
12. Ginsberg JP, Davis RJ, Bennicelli JL, Nauta LE, Barr FG. Up-regulation of MET but not neural cell adhesion molecule expression by the PAX3-FKHR protein in alveolar rhabdomyosarcoma. Cancer Res 1998;58:3542–6.

13. Anderson J, Ramsay A, Gould S, Pritchard-Jones K. PAX3-FKHR induces morphological change and enhances cellular proliferation and invasion in rhabdomyosracoma. Am J Pathol 2001;159:1089–96.
14. Jankowski K, Kucia M, Wysoczynski M, et al. Both hepatocyte growth factor (HGF) and stromal-derived factor-1 regulate the metastatic behavior of human rhabdomyosarcoma cells, but only HGF enhances their resistance to radiochemotherapy. Cancer Res 2003;63: 7926–35.
15. Kami K, Morikawa Y, Kawai Y, Senba E. Leukemia inhibitory factor, glial cell line-derived neurotrophic factor, and their receptor expressions following muscle crush injury. Muscle Nerve 1999;22:1576–86.
16. White JD, Bower JJ, Kurek JB, Austin L. Leukemia inhibitory factor enhances regeneration in skeletal muscles after myoblast transplantation. Muscle Nerve 2001;24:695–7.
17. Kucia M, Dawn B, Hunt G, et al. Cells expressing early cardiac markers reside in the bone marrow and are mobilized into the peripheral blood after myocardial infarction. Circ Res 2004;95:1191–9.
18. Metcalf D. The unsolved enigmas of leukemia inhibitory factor. Stem Cells 2003;21:5–14.
19. Wysoczynski M, Reca R, Ratajczak J, et al. Incorporation of CXCR4 into membrane lipid rafts primes homing-related responses of hematopoietic stem/progenitor cells to an SDF-1 gradient. Blood 2005;105:40–8.
20. Majka M, Janowska-Wieczorek A, Ratajczak J, et al. Numerous growth factors, cytokines, and chemokines are secreted by human CD34(+) cells, myeloblasts, erythroblasts, and megakaryoblasts and regulate normal hematopoiesis in an autocrine/paracrine manner. Blood 2001;97:3075–85.
21. Weigel BJ, Breitfeld PP, Hawkins D, et al. Role of high-dose chemotherapy with hematopoietic stem cell rescue in the treatment of metastatic or recurrent rhabdomyosarcoma. J Pediatr Hematol Oncol 2001;23: 272–6.
22. Mueller A, Homey B, Soto H, et al. Involvement of chemokine receptors in breast cancer metastasis. Nature 2000;410:50–6.
23. Taichman RS, Cooper C, Keller ET, Pienta KJ, Taichman NS, McCauley LK. Use of the stromal cell-derived factor-1/CXCR4 pathway in prostate cancer metastasis to bone. Cancer Res 2002;62:1832–7.
24. Geminder H, Sagi-Assif O, Goldberg L, et al. A possible role for CXCR4 and its ligand, the CXC chemokine stromal cell-derived factor-1, in the development of bone marrow metastases in neuroblastoma. J Immunol 2001;167:4747–57.
25. Ferracini R, Olivero M, DiRenzo MF, et al. Retrogenic expression of the MET proto-oncogene correlates with the invasive phenotype of human rhabdomyosracoma. Oncogene 1996;12:1697–705.
26. Phillips RJ, Burdick MD, Lutz M, et al. The stromal derived factor-1/CXCL12-CXC chemokine receptor 4 biological axis in non-small cell lung cancer metastases. Am J Respir Crit Care Med 2003;167:1676–86.
27. Kijima T, Maulik G, Ma PC, et al. Regulation of cellular proliferation, cytoskeletal function, and signal transduction through CXCR4 and c-Kit in small cell lung cancer cells. Cancer Res 2002;62:6304–11.
28. Lee BC, Lee TH, Avraham S, Avraham HK. Involvement of the chemokine receptor CXCR4 and its ligand stromal cell-derived factor 1α in breast cancer cell migration through human brain microvascular endothelial cells. Mol Cancer Res 2004;2:327–38.
29. Danilkovitch-Miagkova A, Zbar B. Dysregulation of Met receptor tyrosine kinase activity in invasive tumors. J Clin Invest 2002;109:863–7.
30. Mualik G, Shrikhande A, Kijima T, et al. Role of hepatocyte growth factor receptor, c-met, in oncogenesis and potential therapeutic inhibition. Cytokine Growth Factor Rev 2002;13:41–59.
31. Lin S, Rusciano D, Lorenzoni P, et al. C-met activation is necessary but not sufficient for liver colonization by B16 murine melanoma cells. Clin Exp Metastasis 1998;16:253–65.
32. Kucia M, Zhang YP, Reca R, et al. Cells enriched in markers of neural tissue-committed stem cells reside in the bone marrow and are mobilized into the peripheral blood following stroke. Leukemia 2006; 20:18–28.
33. Kami K, Senba E. *In vivo* activation of STAT3 signaling in satellite cells and myofibers in regenerating rat skeletal muscles. J Histochem Cytochem 2002;50: 1579–89.
34. Burridge K, Turner CE, Romer LH. Tyrosine phosphorylation of paxillin and pp125FAK accompanies cell adhesion to extracellular matrix: a role in cytoskeletal assembly. J Cell Biol 1992;119:893–903.
35. Mitra SK, Hanson DA, Schlaepfer DD. Focal adhesion kinase: in command and control of cell motility. Nat Rev Mol Cell Biol 2005;6:56–68.
36. Ng DC, Lin BH, Lim CP, et al. Stat3 regulates microtubules by antagonizing the depolymerization activity of stathmin. J Cell Biol 2006;172:245–57.
37. Epstein JA, Shapiro DN, Cheng J, Lam PYP., Maas RL Pax3 modulates expression of the c-met receptor during limb muscle development. Proc Natl Acad Sci U S A 1996;93:4213–4218.

Leukemia Inhibitory Factor: A Newly Identified Metastatic Factor in Rhabdomyosarcomas

Marcin Wysoczynski, Katarzyna Miekus, Kacper Jankowski, et al.

Cancer Res 2007;67:2131-2140.